Electronic Supplementary Information

Cluster-like Molybdenum Phosphide Anchored on Reduced Graphene Oxide for Efficient Hydrogen Evolution over a Broad pH Range

Haijing Yan,[a] Yanqing Jiao,[a] Aiping Wu,[a] Chungui Tian,*[a] Xiaomeng Zhang,[a] Lei Wang,[a] Zhiyu Ren[a] and Honggang Fu*[a]

[a] *Key Laboratory of Functional Inorganic Material Chemistry, Ministry of Education of the People's Republic of China, Heilongjiang University, Harbin 150080 (China). Email address: chunguitianhq@163.com; fuhg@vip.sina.com;*

The content of ESI

1. Experimental Section

2. Fig. S1 The SEM image of MoP NPs without GO support.
3. Fig. S2 XRD pattern of MoP NPs.
4. Fig. S3 EDX spectrum of MoP/rGO hybrid.
5. Fig. S4 XPS survey spectra of MoP/rGO hybrid.
6. Fig. S5 N_2 adsorption isotherm of the rGO and MoP/rGO hybrids. The inset is the N_2 adsorption isotherm of MoP NPs..
7. Fig. S6 The work function drawings of catalysts, green: MoP/rGO and yellow: Pt black.
8. Fig. S7 XRD pattern of MoO_2/rGO hybrid.
9. Fig. S8 Polarization curves of MoO_2/rGO at pH=0 (a) and 14 (b), respectively.
10. Fig. S9 XRD patterns of MoP/rGO prepared at different temperatures, black: 600 °C and red: 800 °C.
11. Fig. S10 XRD patterns of MoP/rGO with different content of MoP, black: 40% and red: 60%.
12. Fig. S11 Polarization curves of MoP/rGO prepared at different temperatures (600, 700 and 800 °C) at pH=0 and 14, respectively.
13. Fig. S12 Polarization curves of MoP/rGO with different content of MoP (mass ratio: 40%, 50% and 60%) at pH=0 and 14, respectively.
14. Fig. S13 CVs in the region of 0.1-0.2 V with the different rates for MoP/rGO (a) pH=0, (b) pH=14 and MoP (c) pH=0, (d) pH=14.
15. Fig. S14 Exchange current density of catalysts, red : MoP and green: MoP/rGO (a) pH=0, (b) pH=14.

16. Table. S1 BET surface areas of the prepared catalysts.

17. Table S2 The summary of the catalytic performance of MoP/rGO and MoP NPs for HER.

18. Table S3 The summary of the catalytic performance of the different MoP catalysts for HER.

Experimental Section

Chemicals. The $H_3PMo_{12}O_{40}$ (Keggin-type POMs, PMo_{12}), ethanol (C_2H_5OH), sodium hypophosphite (NaH_2PO_2) were purchased from Aladdin Chemical Reagent Co., Ltd. The polyethylenimine (PEI, MW: 600000-1000000) was purchased from Fluka. All regents were used as received without further purification.

Preparation of PMo_{12}/rGO

The PMo_{12}/rGO is prepared by following method. Both of POM anions and GO are negative charges, which are not favorable for their assembly. To make the effective immobilization of PMo_{12} on the GO support, the GO was firstly modified with positive charge immobilized agent (PEI). Typically, the GO sheets (80 mg) were dispersed in water of 20 mL to form a stable dispersion (4 mg mL^{-1}) in an ultrasonic bath for 10 min. The resulted GO dispersion was mixed with 20 mL of 4 mg mL^{-1} PEI aqueous solution under stirring. After the mixed solution was stirred 24 h, the excess immobilized agent was removed by repeated centrifugation (4500 rpm, 5 min) and washing cycles. The PEI-GO was dispersed in deionized (DI) water for compounding with PMo_{12} (mass ratio of PMo_{12} on the GO is 50%). For comparison, the other mass ratio of 40% and 60% were also prepared. To anchor the PMo_{12} on PEI-GO, a certain amount of PMo_{12} in deionized water (40 mL) was dropwise added into the PEI-GO solution of 40 mL (2 mg mL^{-1}) under vigorously stirring. After stirring for 24 h, the mixture was transferred into a 100 mL Telfon-lined autoclave and hydrothermally treated at 180 °C for 10 h. The resulting solid (black) was collected by centrifugation and washing repeatedly with DI water and alcohol. The hydrothermal treatment can result in the reduction of GO to rGO.

Preparation of MoP/rGO

In the synthesis, 50 mg PMo_{12}/rGO was firstly calcined at 300 °C for 5 h. Then the sample after calcination and NaH_2PO_2 (1.5g) were putted into two separate porcelain boats with NaH_2PO_2 at the upstream side of the furnace. Subsequently, the samples were heated at 700 °C with a heating rate of 5 °C min^{-1} and maintained at 700 °C for 3 h, and then naturally cooled to ambient temperature under N_2. Moreover, the MoO_2/rGO sample was prepared using the same method without introducing of NaH_2PO_2. For comparison, the other calcining temperatures (600 and 800 °C) were also preformed.

Electrode preparation and electrochemical measurements

Electrochemical measurements were performed with a BAS100B electrochemical workstation. A three-electrode configuration at room temperature was used, where glassy carbon electrode (GCE), carbon rod and Hg/Hg_2Cl_2 (saturated KCl-filled) were used as the work electrode, the auxiliary electrode and the reference electrode, respectively. All the potentials were recorded with respect to the reversible hydrogen electrode (RHE). Catalyst ink was typically made by dispersing 5 mg of catalyst in 1 mL water/ethanol mixture (v/v=4:1). After adding 50 μL of 5 wt % of Nafion solution and ultrasonication, an aliquot of 5 μL was pipetted onto the GCE (0.07065 cm^2) to reach the catalyst loading of 0.337 mg cm^{-2}. Current density was normalized to the geometrical area of the working electrode. Polarization data was collected in 0.5 M H_2SO_4 and 1M KOH with the scan rate of 5 mV s^{-1} on the GCE under 1600 rpm. The ESCA of the catalysts modified electrodes were calculated using the double-layer capacitor using reported electrochemical method. The cyclic voltammograms (CVs) were tested with different rates from 20 to 200 mV s^{-1}. For long-term stability tests, which were carried out at 100 mV s^{-1}. The pH of the testing solution was measured before and after testing with no change observed.

Physical Characterizations

The morphology and structure of the samples were analyzed by scanning electron microscopy (SEM: Hitachi S-4800) with an acceleration voltage of 5 kV and transmission electron microscopy (TEM: JEM-2100) with an acceleration voltage of 200 kV. Carbon-coated copper grids were used as sample holders for TEM analysis. XPS (X-ray photoelectron spectroscopy) analysis was performed on a VG ESCALABMK II with a Mg Kα achromatic X-ray source (1253.6 eV). X-ray diffraction (XRD) patterns were obtained on a Bruke D8 diffractometer using Cu K_α (λ=1.5406 Å) radiation. The accelerating voltage and the applied current were 40 kV and 20 mA, respectively. Raman measurement was performed with a Jobin Yvon HR 800 micro-Raman spectrometer at 457.9 nm. Thermogravimetric analysis was performed on a TA-Q600 thermal analyzer with a heating rate of 10 K min^{-1} under air. The N_2 adsorption-desorption isotherms of as-made samples were conducted by using a Micromeritics Tristar II. The samples were outgassed for 10 h at 150 °C under vacuum before the measurements. Scanning Kelvin probe (SKP) measurements (SKP5050 system, Scotland) were performed at normal laboratory conditions (in ambient atmosphere). A gold electrode was used as the reference electrode.

The chemistry used for immobilization and the support:

In our synthesis, the graphene oxide (GO) obtained by the Hummer's method was selected as the catalytic support based on their virtues of easily preparation in large quality and easily assembly with many particles owing to their abundant functional groups (hydroxyl and carboxyl). While the direct growth of POMs on GO will result in the formation of uneven particles because the negative charges of both POM anions and the GO are not favorable for the assembly of them. To overcome this problem, the GO was first modified with polyethyleneimine (PEI), consisting of numerous positive charges, which guarantees its easy manipulation as a substrate for PMo_{12}. Then, PMo_{12} clusters were anchored on PEI-modified GO using the electrostatic assembly through a hydrothermal process. Due to the intensive interaction of negative charged PMo12 anions and positive charged PEI-modified GO, the PMo_{12} clusters can be tightly immobilized on the GO with small size and well dispersion. Benefiting from the strong immobilizing effects, after following calcining in air (for easily converting to phosphides) and then phosphatizing, the MoP NPs could maintain the ultrasmall size (3 nm) and uniform distribution.

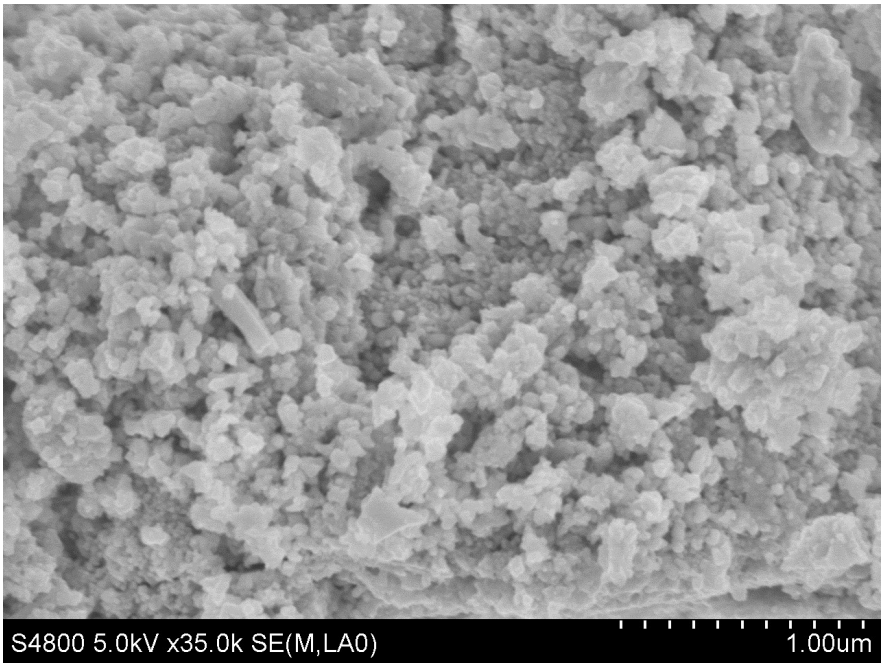

Fig. S1 The SEM image of MoP NPs without GO support. It can be seen that the MoP NPs are about 200~500 nm in size, indicating that rGO is key to the confined generation of particles to obtain the small sized, cluster-like MoP.

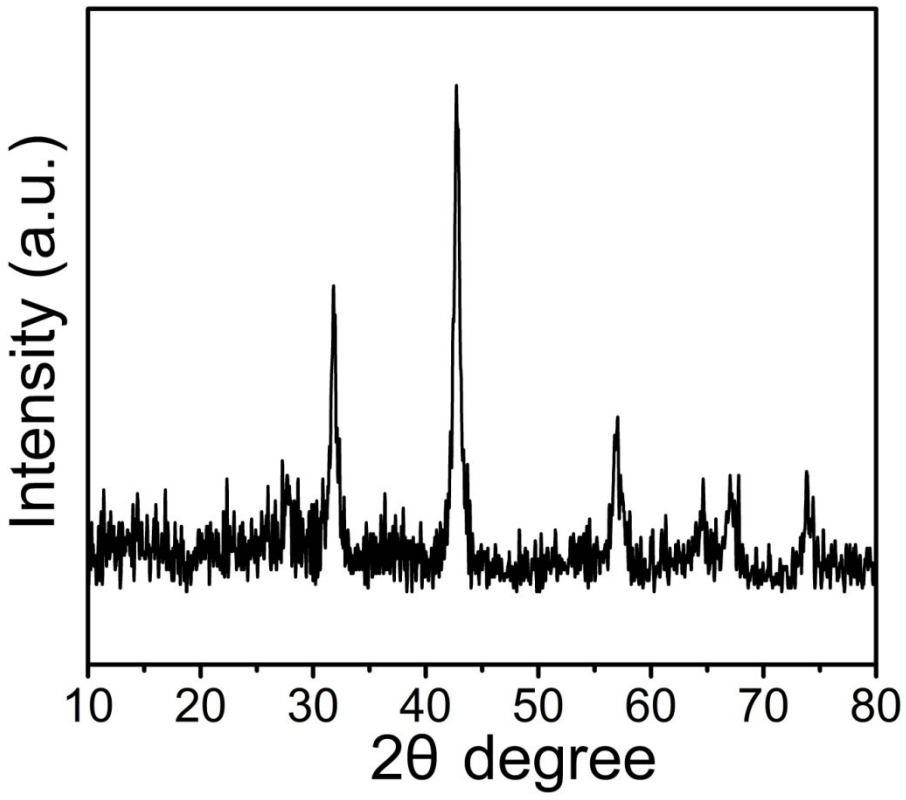

Fig. S2 XRD pattern of MoP NPs. It can be seen that the XRD peaks of MoP NPs are narrow and strong, demonstrating the large size of particles which is agreement with SEM result.

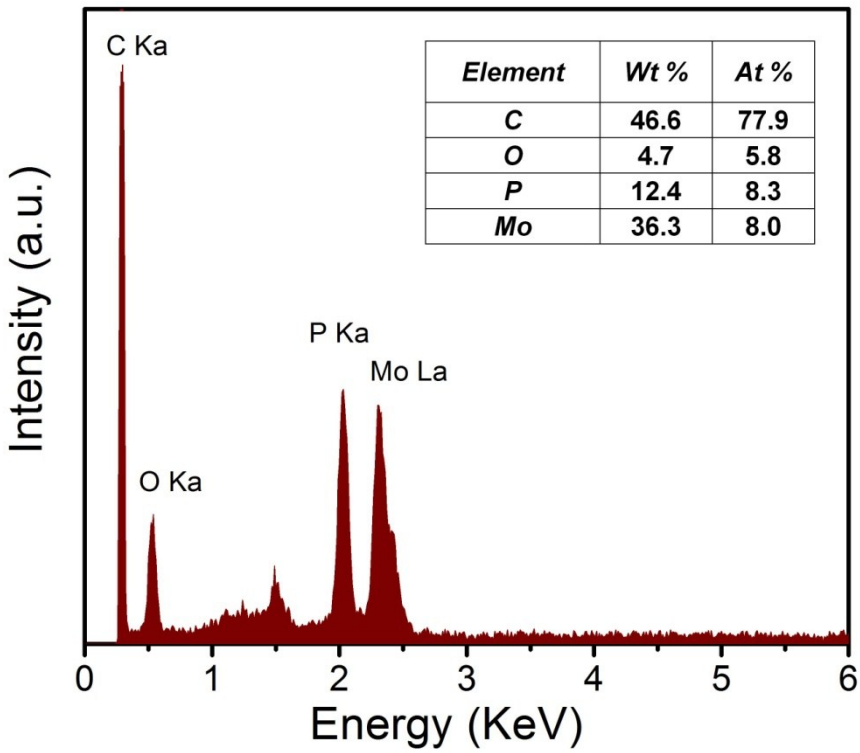

Element	Wt %	At %
C	46.6	77.9
O	4.7	5.8
P	12.4	8.3
Mo	36.3	8.0

Fig. S3 EDX spectrum of MoP/rGO hybrid.

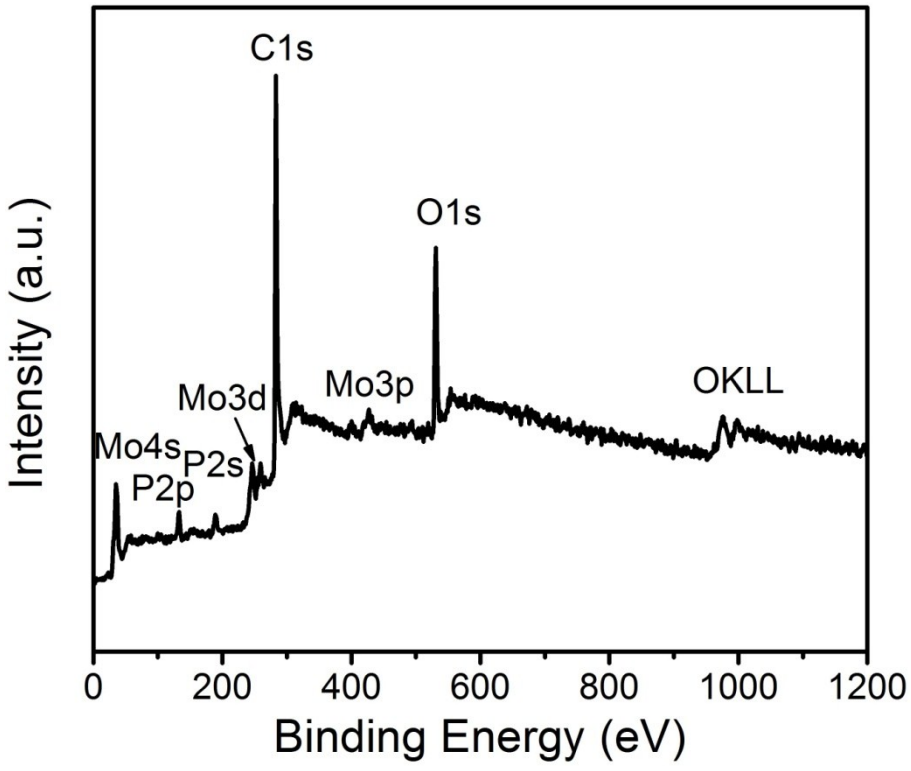

Fig. S4 XPS survey spectra of MoP/rGO hybrid. The result reveals that the MoP/rGO is mainly composed of C, P, O and Mo elements.

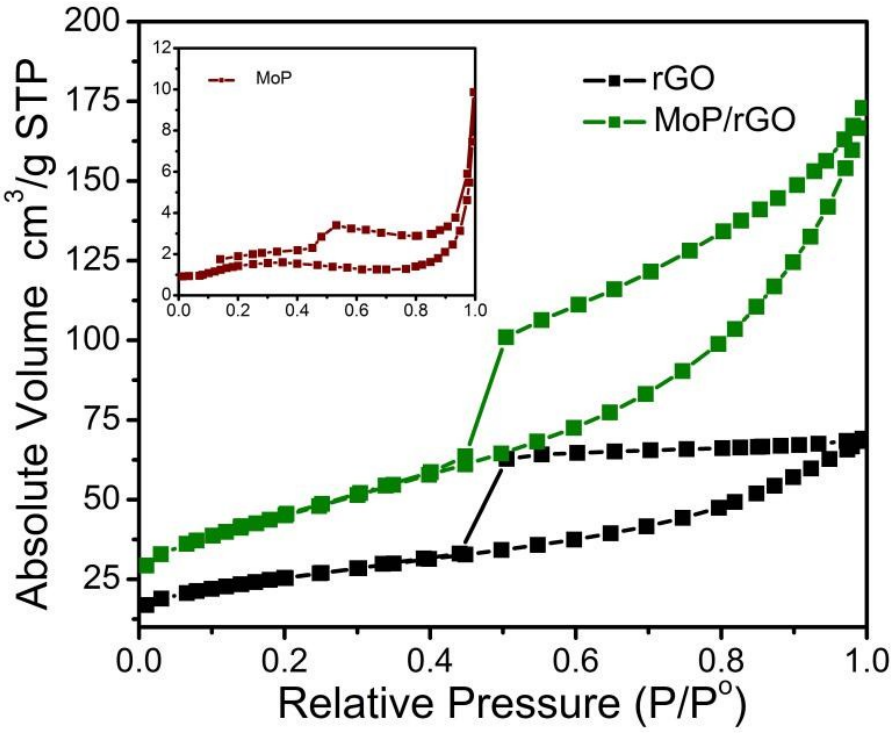

Fig. S5 N_2 adsorption isotherm of the rGO and MoP/rGO hybrids. The inset is the N_2 adsorption isotherm of MoP NPs..

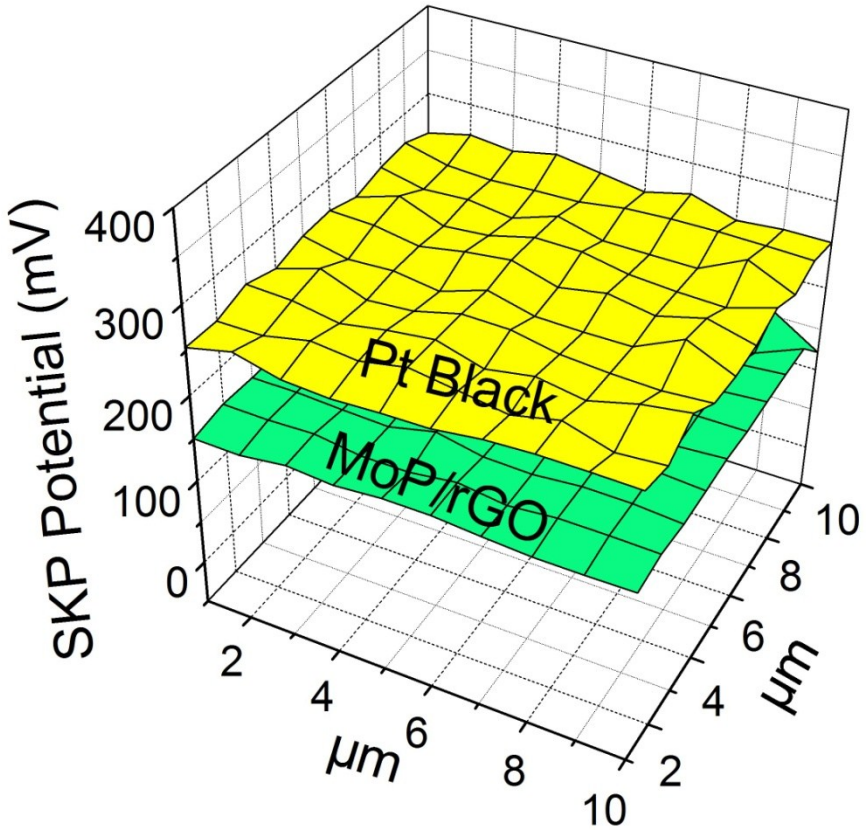

Fig. S6 The work function drawings of catalysts, green: MoP/rGO and yellow: Pt black. The WF values of the MoP/rGO and Pt black are about 5.5 eV and 5.60 eV, respectively.

The platinum metal has excellent catalytic properties for the HER owing to its high WF, which is favorable to trap electrons. As we can see, the WF value of MoP/rGO is 5.5 eV, which is close to that of Pt (5.6 eV), implying the MoP/rGO as promising like-Pt catalyst for HER.

The work function (φ) is calculated by formula S1:

$$\varphi_{Au} - \frac{\eta_{Au}}{1000} = \varphi - \frac{\eta}{1000}$$

in which φ_{Au} is the work function of Au, η_{Au}= -239.75 eV.

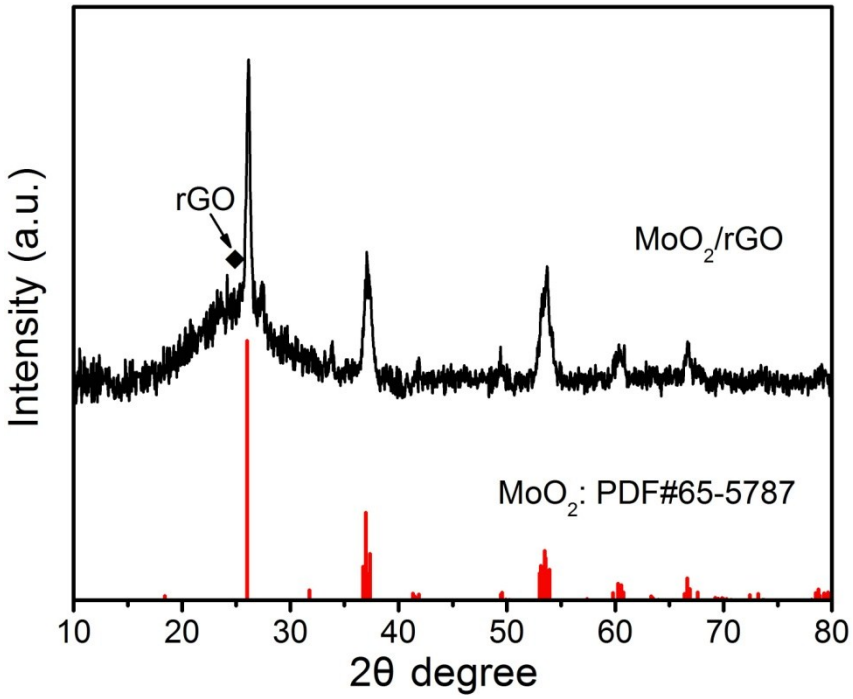

Fig. S7 XRD pattern of MoO_2/rGO hybrid.

In the XRD pattern of MoO_2/rGO hybrid, the wide peak at 26.5° is indexed to the (002) reflection of hexagonal graphite and the other peaks are assigned to monoclinic MoO_2 (PDF#65-5787).

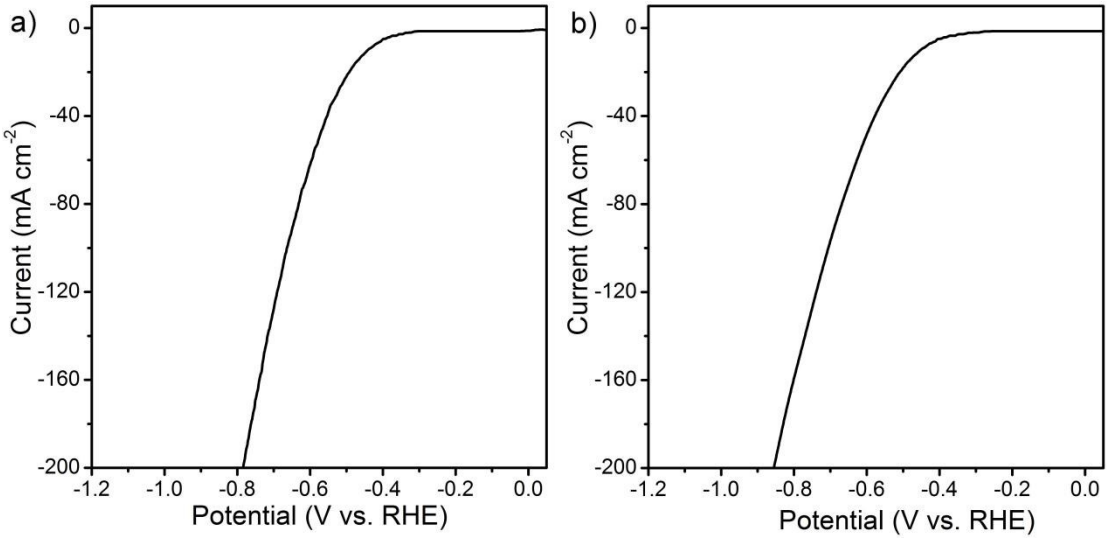

Fig. S8 Polarization curves of MoO_2/rGO at pH=0 (a) and 14 (b), respectively.

The MoO_2/rGO had onset potential of 301 mV (pH=0) and 237 mV (pH=14) and achieves the current densities of 10 mA cm^{-2} at the overpotential of 439 (pH=0) and 445 mV (pH=14), which are much lower than that of MoP/rGO.

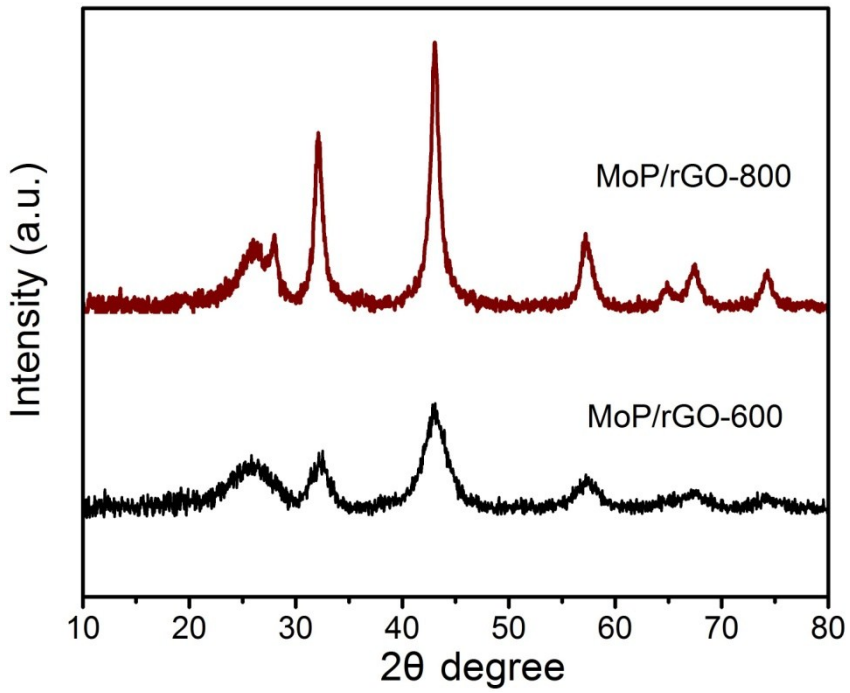

Fig. S9 XRD patterns of MoP/rGO prepared at different temperatures, black: 600 °C and red: 800 °C.

The XRD peaks of MoP in the MoP/rGO are becoming narrow and strong with the increase of temperature by the combination of MoP/rGO prepared at 700°C. The result indicates the improvement of crystallinity and the increase of particle size with the increase of the temperature.

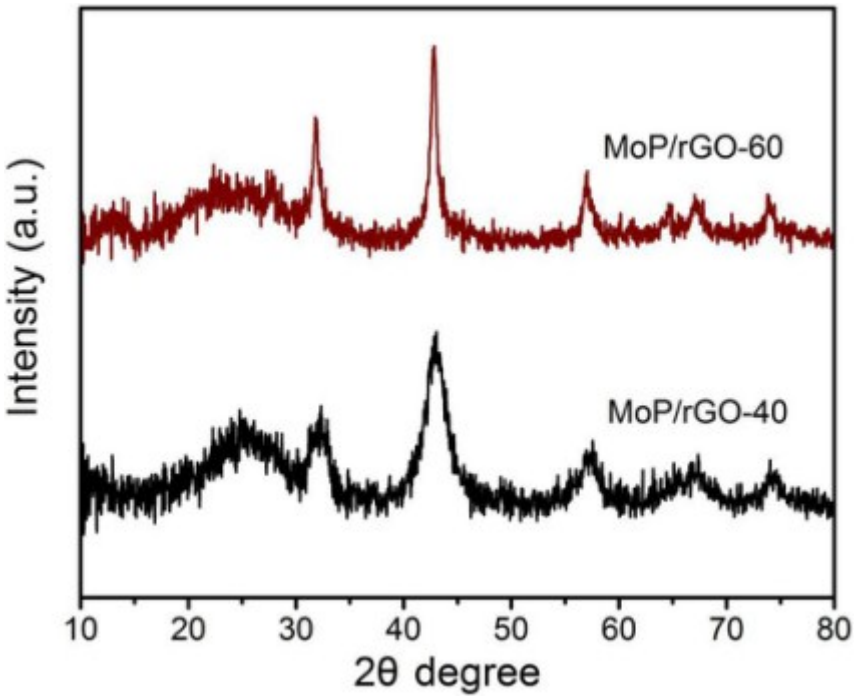

Fig. S10 XRD patterns of MoP/rGO with different content of MoP, black: 40% and red: 60%. The amount of MoP was calculated based on the mass of PMo_{12} adding in the begin of synthesis.

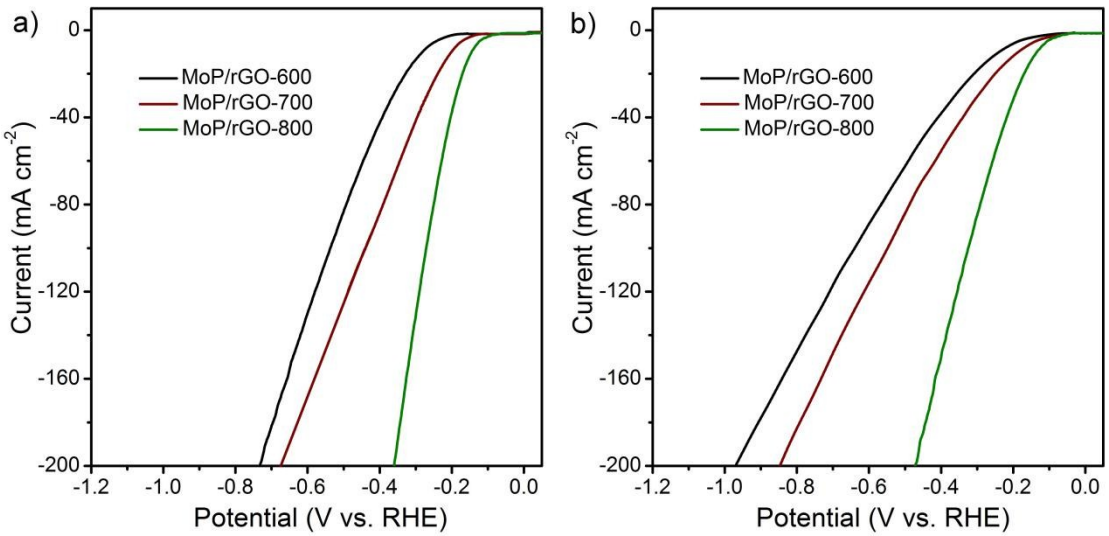

Fig. S11 Polarization curves of MoP/rGO prepared at different temperatures (600, 700 and 800 °C) at pH=0 and 14, respectively.

As can be seen, the MoP/rGO prepared at 700 °C has the best catalytic activity. This result shows that the small particle size and appropriate crystallinity are of importance for enhanced catalytic activity of MoP/rGO.

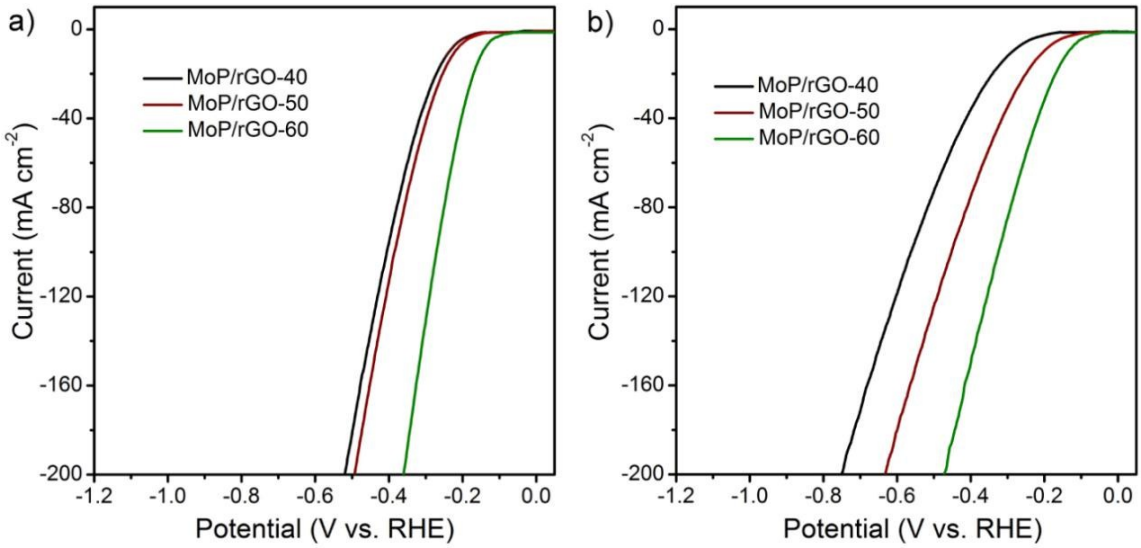

Fig. S12 Polarization curves of MoP/rGO with different content of MoP (mass ratio: 40%, 50% and 60%) at pH=0 and 14, respectively.

When the mass ratio of MoP on the rGO is 50%, the MoP/rGO exhibits the best HER activity. This result shows that appropriate ratio of rGO and MoP is also important factor that affects the performance of MoP materials.

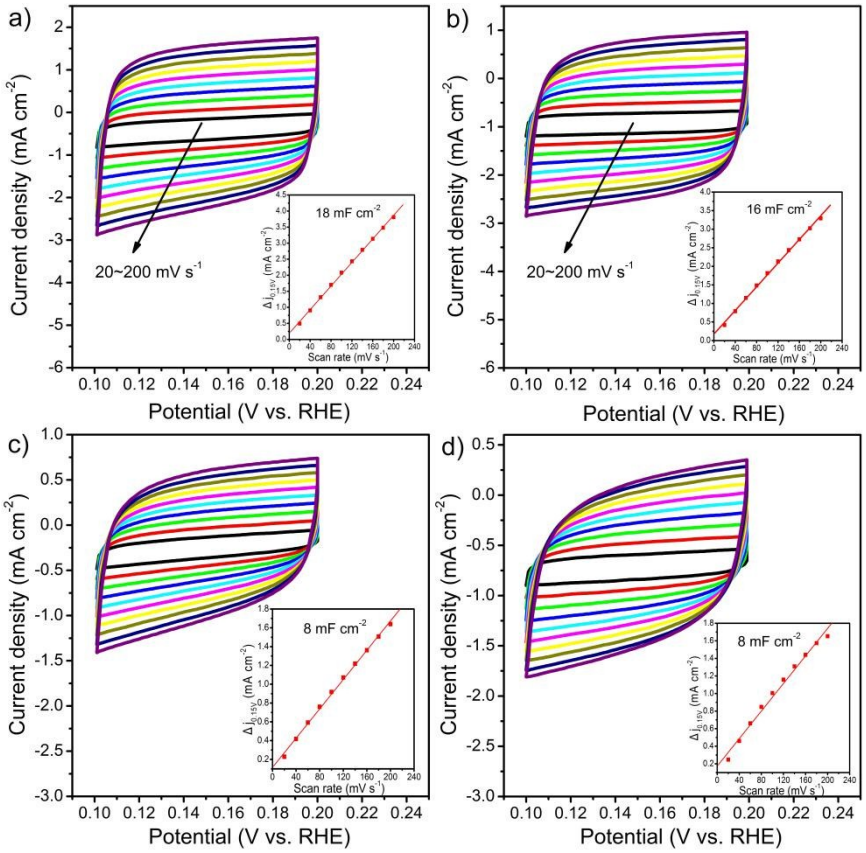

Fig. S13 CVs in the region of 0.1-0.2 V with the different rates for MoP/rGO (a) pH=0, (b) pH=14 and MoP (c) pH=0, (d) pH=14. The inset is the capacitive current at 0.15 V as a function of scan rate for MoP/rGO and MoP, respectively.

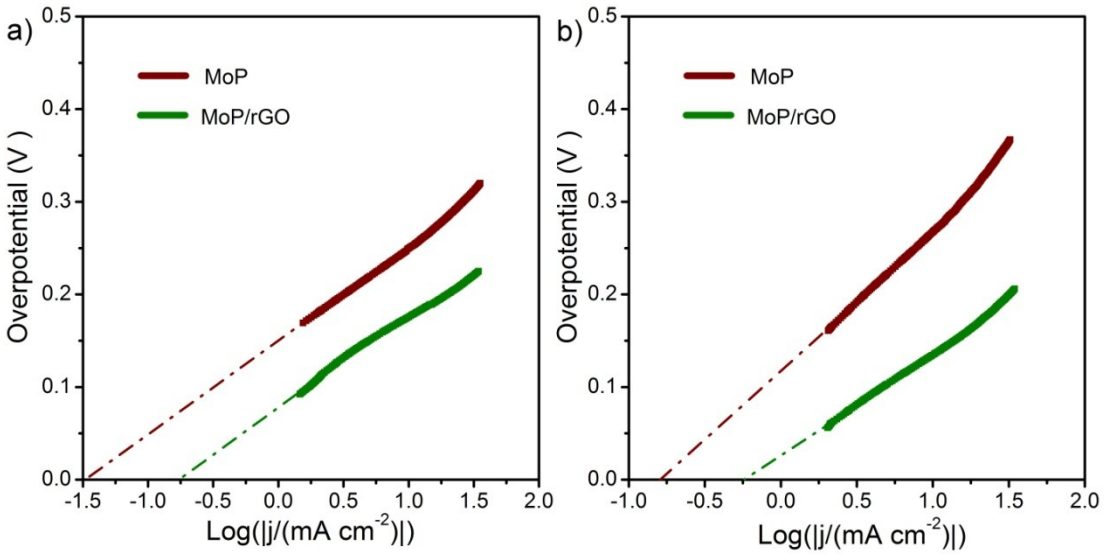

Fig. S14 Exchange current density of catalysts, red: MoP and green: MoP/rGO (a) pH=0, (b) pH=14.

Table. S1 BET surface areas of the prepared catalysts

Catalysts	$S_{BET}(m^2\ g^{-1})$
MoP/rGO	**160.2**
rGO	**72.9**
MoP	**5.4**

Table S2 The summary of the catalytic performance of MoP/rGO and MoP NPs for HER.

Entry	Catalysts	pH	Onset η (mV)	Tafel slope (mV dec^{-1})	η_{10} (mV)	j_0 (mA cm^{-2})
1	**MoP/rGO**	**0**	**16**	**58**	**119**	**0.178**
2	**MoP**	**0**	**119**	**65**	**225**	**0.035**
3	**MoP/rGO**	**14**	**22**	**72**	**140**	**0.578**
4	**MoP**	**14**	**135**	**105**	**276**	**0.164**

Table S3 The summary of the catalytic performance of the different MoP catalysts for HER.

Catalysts, loading (mg cm^{-2})	Particle size	Onset η (mV)	η_{10} (mV)	Tafel slope (mV dec^{-1})	j_0 (mA cm^{-2})	Conditions (electrolyte)	Ref.
Closely Interconnected Network MoP (0.36)	20 nm	40	125	54	8.6×10^{-2}	0.5 M H_2SO_4	**S1**
3D MoP sponge (0.35)	>50 nm	-	105	126	3.05	0.5 M H_2SO_4	**S2**
Amorphous MoP-Ti foil (1)	4 nm	50	110	45	1.2×10^{-4}	0.5 M H_2SO_4	**S3**
MoP-porous carbon (0.243)	30-50 nm	63	126	63	1.44×10^{-4}	0.5 M H_2SO_4	**S4**
Bulk MoP (0.071)	50 nm	110	246	60	4.15×10^{-3}	0.5 M H_2SO_4	**S5**
MoP-graphite Nanosheets (0.64)	9 nm	100	300	63	1.2×10^{-3}	0.5 M H_2SO_4	**S6**
Bulk MoP (0.86)	1-2 μm	50	-	54	3.4×10^{-2}	0.5 M H_2SO_4	**S7**
Electrochemically activated MoP (0.1)	0.5-1 μm	100	150	50	-	0.5M H_2SO_4	**S8**
		110	190	-	-	1 M KOH	
Cluster-like MoP/rGO (0.337)	**3 nm**	**16**	**119**	**58**	**1.78×10^{-1}**	**0.5 M H_2SO_4**	**This work**
		22	**140**	**72**	**5.78×10^{-1}**	**1 M KOH**	

From Table S3, we can see that the MoP/rGO shows superior activity to the most reported MoP-based catalysts, especially in the values of onset potential.

In addition, we can find that the amorphous MoP-Ti foil (4 nm) show better performance than cluster-like MoP/rGO in terms of Tafel slope in acid media. As we known, the catalytic performance of catalyst can also be affected by the catalyst loading in test.[S9,S10] A high loading would be favorable to improve the performance of the catalysts, such as lowing Tafel slope and enhancing the current density at certain η. The loading of amorphous MoP-Ti foil (4 nm) (1 mg cm^{-2}) is much higher than that of cluster-like MoP/rGO on electrode is about 0.337 mg cm^{-2}, which should be important reason to show better performance of the catalyst. In another word, the performance of ultrasmall and highly uniform MoP/rGO can be further improved by growth of

them on suitable supports with high loading (Ti plate etc.)

References

S1 Z. Xing, Q. Liu, A. M. Asiri and X. Sun, *Adv. Mater.*, 2014, **26**, 5702-5707.

S2 C. Deng, F. Ding, X. Y. Li, Y. F. Guo, W. Ni, H. Yan, K. N. Sun and Y. M. Yan, *J. Mater. Chem. A*, 2016, **4**, 59-66.

S3 J. M. McEnaney, J. C. Crompton, J. F. Callejas, E. J. Popczun, A. J. Biacchi, N. S. Lewis and R. E. Schaak, *Chem. Mater.,* 2014, **26**, 4826-4831.

S4 Z. Q. Yao, Y. Z. Su, C. B. Lu, C. Q. Yang, Z. X. Xu, J. H. Zhu, X. D. Zhuang and F. Zhang, *New J. Chem.*, 2016, DOI: 10.1039/c5nj03440j.

S5 B. Chen, D. Z. Wang, Z. P. Wang, P. Zhou, Z. Z. Wu and F. Jiang, *Chem. Commun.*, 2014, **50**, 11683-11685.

S6 S. J. Aravind, K. Ramanujachary, A. Mugweru and T. D. Vaden, *Appl. Catal. A: Gen.*, 2015, **490**, 101-107.

S7 Xiao, M. A. Sk, L. Thia, X. M. Ge, R. J. Lim, J. Y. Wang, K. H. Lim and X. Wang, *Energy Environ. Sci.*, 2014, **7**, 2624-2629.

S8 T. Y. Wang, K. Z. Du, W. L. Liu, Z. W. Zhu, Y. H. Shao and M. X. Li, *J. Mater. Chem. A*, 2015, **3**, 4368-4373.

S9 J. Q. Tian, Q. Liu, A. M. Asiri and X. P. Sun, *J. Am. Chem. Soc.*, 2014, **136**, 7587-7590.

S10 J. Kibsgaard and T. F. Jaramillo, *Angew. Chem. Int. Ed.*, 2014, **53**, 14433-14437.